

Selection of material and shape

7.1 Introduction and synopsis

Shaped sections carry bending, torsional and axial-compressive loads more efficiently than solid sections do. By ‘shaped’ we mean that the cross-section is formed to a tube, a box-section, an I-section or the like. By ‘efficient’ we mean that, for given loading conditions, the section uses as little material, and is therefore as light, as possible. Tubes, boxes and I-sections will be referred to as ‘simple shapes’. Even greater efficiencies are possible with sandwich panels (thin load-bearing skins bonded to a foam or honeycomb interior) and with structures (the Warren truss, for instance).

This chapter extends the concept of indices so as to include shape (Figure 7.1). Often it is not necessary to do so: in the case studies of Chapter 6, shape either did not enter at all, or, when it did, it was not a variable (that is, we compared materials with the same shape). But when two materials are available with different section shapes and the design is one in which shape matters (a beam in bending, for example), the more general problem arises: how to choose, from among the vast range of materials and the section shapes in which they are available — or could, potentially, be made — the one which maximizes the performance. Take the example of a bicycle: its forks are loaded in bending. It could, say, be made of steel or of wood — early bikes *were* made of wood. But steel is available as thin-walled tube, whereas the wood is not; wood, usually, has a solid section. A solid wood bicycle is certainly lighter and stiffer than a solid steel one, but is it better than one made of steel tubing? Might a magnesium I-section be better still? What about a webbed polymer moulding? How, in short, is one to choose the best combination of material and shape?

A procedure for answering these and related questions is outlined in this chapter. It involves the definition of *shape factors*: simple numbers which characterize the efficiency of shaped sections. These allow the definition of material indices which are closely related to those of Chapter 5, but which now include shape. When shape is constant, the indices reduce exactly to those of Chapter 5; but when shape is a variable, the shape factor appears in the expressions for the indices.

The ideas in this chapter are a little more difficult than those of Chapter 5; their importance lies in the connection they make between materials selection and the designs of load-bearing structures. A feel for the method can be had by reading the following section and the final section alone; these, plus the results listed in Tables 7.1 and 7.2, should be enough to allow the case studies of Chapter 8 (which apply the method) to be understood. The reader who wishes to grasp how the results arise will have to read the whole thing.

7.2 Shape factors

As explained in Chapter 5, the loading on a component is generally axial, bending or torsional: *ties* carry tensile loads; *beams* carry bending moments; *shafts* carry torques; *columns* carry compressive

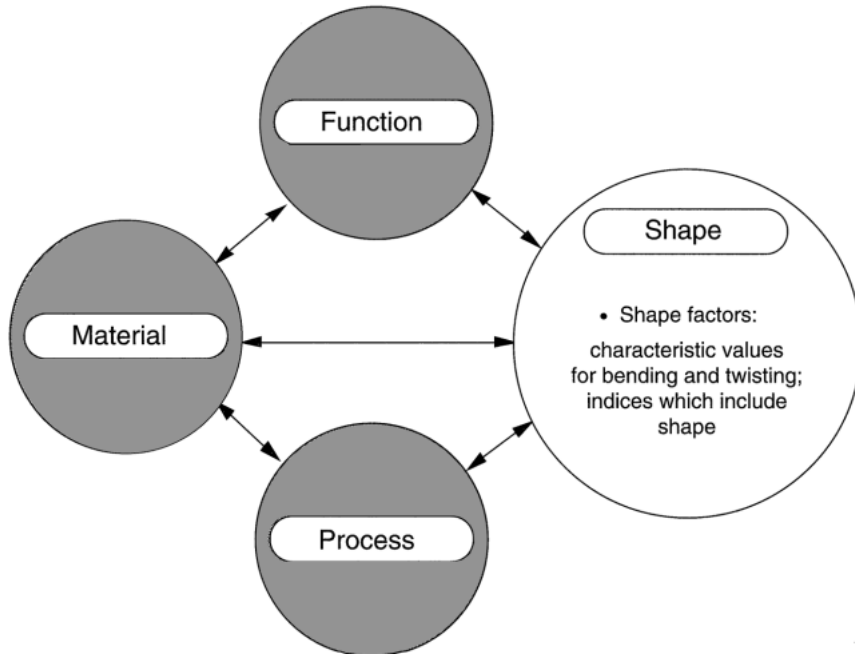


Fig. 7.1 Section shape is important for certain modes of loading. When shape is a variable a new term, the shape factor, appears in some of the material indices: they then allow optimum selection of material and shape.

axial loads. Figure 7.2 shows these modes of loading, applied to shapes that resist them well. The point it makes is that the best material-and-shape combination depends on the mode of loading. In what follows, we separate the modes, dealing with each separately.

In axial tension, the area of the cross-section is important but its shape is not: all sections with the same area will carry the same load. Not so in bending: beams with hollow-box or I-sections are better than solid sections of the same cross-sectional area. Torsion too, has its 'best' shapes: circular tubes, for instance, are better than either solid sections or I-sections. To deal with this, we define a *shape factor* (symbol ϕ) which measures, for each mode of loading, the efficiency of a shaped section. We need four of them, which we now define.

A *material* can be thought of as having properties but no shape; a *component* or a *structure* is a material made into a shape (Figure 7.3). A *shape factor* is a dimensionless number which characterizes the efficiency of the shape, regardless of its scale, in a given mode of loading. Thus there is a shape factor, ϕ_B^e , for elastic bending of beams, and another, ϕ_T^e , for elastic twisting of shafts (the superscript e means elastic). These are the appropriate shape factors when design is based on stiffness; when, instead, it is based on strength (that is, on the first onset of plastic yielding or on fracture) two more shape factors are needed: ϕ_B^f and ϕ_T^f (the superscript f meaning failure). All four shape factors are defined so that they are equal to 1 for a solid bar with a circular cross-section.

Elastic extension (Figure 7.2(a))

The elastic extension or shortening of a tie or strut under a given load (Figure 7.2(a)) depends on the area A of its section, but not on its shape. No shape factor is needed.

Table 7.1 Moments of areas of sections for common shapes

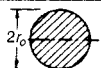
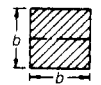
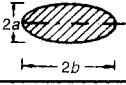
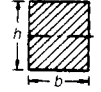
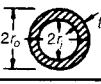
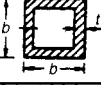
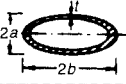
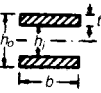
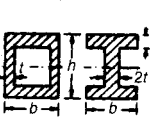
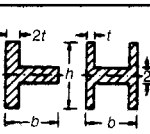
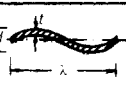
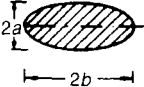
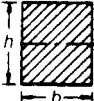
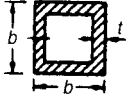
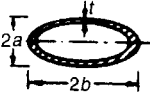
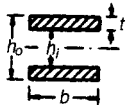
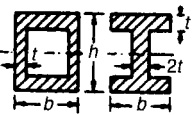
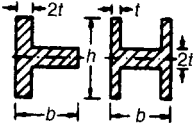
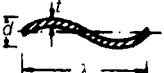
Section Shape	$A(m^2)$	$I_{xx}(m^4)$	$K(m^4)$	$Z(m^3)$	$Q(m^3)$
	πr^2	$\frac{\pi}{4} r^4$	$\frac{\pi}{2} r^4$	$\frac{\pi}{4} r^3$	$\frac{\pi}{2} r^3$
	b^2	$\frac{b^4}{12}$	$0.14b^4$	$\frac{b^3}{6}$	$0.21b^3$
	πab	$\frac{\pi}{4} a^3 b$	$\frac{\pi a^3 b^3}{(a^2 + b^2)}$	$\frac{\pi}{4} a^2 b$	$\frac{\pi a^2 b}{2}$ ($a < b$)
	bh	$\frac{bh^3}{12}$	$\frac{b^3 h}{3} \left(1 - 0.58 \frac{b}{h}\right)$ ($h > b$)	$\frac{bh^2}{6}$	$\frac{b^2 h^2}{3h + 1.8b}$ ($h > b$)
	$\frac{\sqrt{3}}{4} a^2$	$\frac{a^4}{32\sqrt{3}}$	$\frac{a^4 \sqrt{3}}{80}$	$\frac{a^3}{32}$	$\frac{a^3}{20}$
	$\pi(r_o^2 - r_i^2)$ $\approx 2\pi r t$	$\frac{\pi}{4}(r_o^4 - r_i^4)$ $\approx \pi r^3 t$	$\frac{\pi}{2}(r_o^4 - r_i^4)$ $\approx 2\pi r^3 t$	$\frac{\pi}{4r_o}(r_o^4 - r_i^4)$ $\approx \pi r^2 t$	$\frac{\pi}{2r_o}(r_o^4 - r_i^4)$ $\approx 2\pi r^2 t$
	$4bt$	$\frac{2}{3} b^3 t$	$b^3 t \left(1 - \frac{t}{b}\right)^4$	$\frac{4}{3} b^2 t$	$2b^2 t \left(1 - \frac{t}{b}\right)^2$
	$\pi(a + b)t$	$\frac{\pi}{4} a^3 t \left(1 + \frac{3b}{a}\right)$	$\frac{4\pi(ab)^{5/2} t}{(a^2 + b^2)}$	$\frac{\pi a^2 t}{4} \left(1 + \frac{3b}{a}\right)$	$2\pi t(a^3 b)^{1/2}$ ($b > a$)
	$b(h_o - h_i)$ $\approx 2bt$	$\frac{b}{12}(h_o^3 - h_i^3)$ $\approx \frac{1}{2} bth_o^2$	—	$\frac{b}{6h_o}(h_o^3 - h_i^3)$ $\approx bth_o$	—
	$2t(h + b)$	$\frac{1}{6} h^3 t \left(1 + \frac{3b}{h}\right)$	$\frac{2tb^2 h^2}{h + b}$ I $\frac{2}{3} bt^3 \left(1 + \frac{4h}{b}\right)$ □	$\frac{h^2 t}{3} \left(1 + \frac{3b}{h}\right)$	$2tbh$ I $\frac{2}{3} bt^2 \left(1 + \frac{4h}{b}\right)$ □
	$2t(h + b)$	$\frac{t}{6}(h^3 + 4bt^2)$	$\frac{t^3}{3}(8b + h)$ H $\frac{2}{3} ht^3 \left(1 + \frac{4b}{h}\right)$ ┌	$\frac{t}{3h}(h^3 + 4bt^2)$	$\frac{t^2}{3}(8b + h)$ H $\frac{2}{3} ht^2 \left(1 + \frac{4b}{h}\right)$ ┌
	$t\lambda \left(1 + \frac{\pi^2 d^2}{4\lambda^2}\right)$	$\frac{t\lambda d^2}{8}$	—	$\frac{t\lambda d}{4}$	—

Table 7.2 Values for the four shape factors

Section shape	Stiffness		Strength	
	ϕ_B^c	ϕ_T^c	ϕ_B^f	ϕ_T^f
	1	1	1	1
	$\frac{\pi}{3} = 1.05$	0.88	$\frac{2}{3}\sqrt{\pi} = 1.18$	0.74
	$\frac{a}{b}$	$\frac{2ab}{(a^2 + b^2)}$	$\sqrt{\frac{a}{b}}$	$\sqrt{\frac{a}{b}}$ ($a < b$)
	$\frac{\pi h}{3 b}$	$\frac{2\pi b}{3 h} \left(1 - 0.58 \frac{b}{h}\right)$ ($h > b$)	$\frac{2}{3}\sqrt{\pi} \left(\frac{h}{b}\right)^{1/2}$	$\frac{2}{3}\sqrt{\pi} \frac{(b/h)^{1/2}}{(1 + 0.6b/h)}$ ($h > b$)
	$\frac{2\pi}{3\sqrt{3}} = 1.21$	$\frac{2\pi}{5\sqrt{3}} = 0.73$	0.77	0.62
	$\frac{r}{t}$	$\frac{r}{t}$	$\left(\frac{2r}{t}\right)^{1/2}$	$\left(\frac{2r}{t}\right)^{1/2}$

(continued overleaf)

Table 7.2 (continued)

Section shape	ϕ_B^c	Stiffness	ϕ_T^c	ϕ_B^f	Strength	ϕ_T^f
	$\frac{\pi b}{6 t}$		$\frac{\pi b}{8 t} \left(1 - \frac{t}{b}\right)^4$	$\frac{2}{3} \sqrt{\pi} \left(\frac{b}{t}\right)^{1/2}$		$\frac{\sqrt{\pi}}{2} \left(\frac{b}{t}\right)^{1/2} \left(1 - \frac{t}{b}\right)^2$
	$\frac{a(1+3b/a)}{t(1+b/a)^2}$		$\frac{8(ab)^{5/2}}{t(a^2+b^2)(a+b)^2}$	$\left(\frac{a}{t}\right)^{1/2} \frac{(1+3b/a)}{(1+b/a)^{3/2}}$		$\frac{4a^{1/2}}{t^{1/2}(1+a/b)^{3/2}}$
	$\frac{\pi h^2}{2 b t}$		—	$\sqrt{2\pi} \frac{h}{(b t)^{1/2}}$		—
	$\frac{\pi h(1+3b/h)}{6 t(1+b/h)^2}$		$\frac{\pi b^2 h^2}{t(h+b)^3}$	$\frac{\sqrt{2\pi} \left(\frac{h}{t}\right)^{1/2} (1+3b/h)}{3(1+b/h)^{3/2}}$		$\frac{\sqrt{2\pi} h}{(b t)^{1/2} (1+h/b)^{3/2}}$
			$\frac{\pi t(1+4h/b)}{3 b(1+h/b)^2}$			$\frac{\sqrt{2\pi} \left(\frac{t}{b}\right)^{1/2} (1+4h/b)}{3(1+h/b)^{3/2}}$
	$\frac{\pi h(1+4b t^2/h^3)}{6 t(1+b/h)^2}$		$\frac{\pi t(1+8b/h)}{6 h(1+b/h)^2}$	$\frac{\sqrt{\pi} \left(\frac{h}{t}\right)^{1/2} (1+4b t^2/h^3)}{2(1+b/h)^{3/2}}$		$\left(\frac{\pi t}{18 h}\right)^{1/2} \frac{(1+8b/h)}{(1+b/h)^{3/2}}$
			$\frac{\pi t(1+4b/h)}{3 h(1+b/h)^2}$			$\frac{\sqrt{2\pi} \left(\frac{t}{h}\right)^{1/2} (1+4b/h)}{3(1+b/h)^{3/2}}$
	$\frac{\pi d^2}{2 t \lambda}$		—	$\sqrt{\pi} \frac{d}{(t \lambda)^{1/2}}$		—

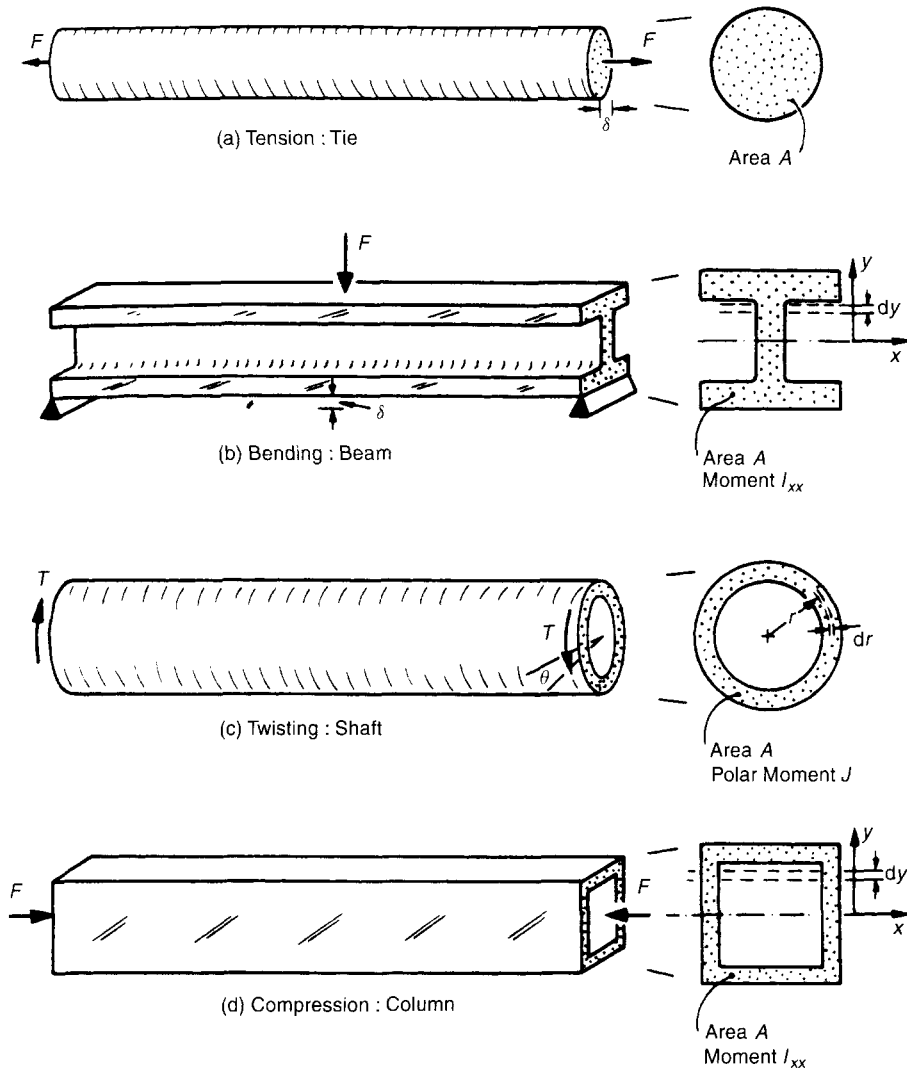


Fig. 7.2 Common modes of loading: (a) axial tension; (b) bending; (c) torsion; and (d) axial compression, which can lead to buckling.

Elastic bending and twisting (Figure 7.2(b) and (c))

If, in a beam of length ℓ , made of a material with Young's modulus E , shear is negligible, then its bending stiffness (a force per unit displacement) is

$$S_B = \frac{C_1 EI}{\ell^3} \tag{7.1}$$

where C_1 is a constant which depends on the details of the loading (values are given in Appendix A, Section A3). Shape enters through the second moment of area, I , about the axis of bending

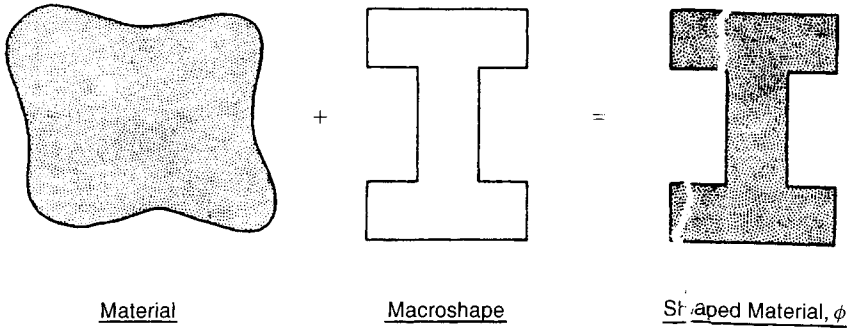


Fig. 7.3 Mechanical efficiency is obtained by combining material with macroscopic shape. The shape is characterized by a dimensionless shape factor, ϕ . The schematic is suggested by Parkhouse (1987).

(the x axis):

$$I = \int_{\text{section}} y^2 dA \tag{7.2}$$

where y is measured normal to the bending axis and dA is the differential element of area at y . Values of I and of the area A for common sections are listed in Table 7.1. Those for the more complex shapes are approximate, but completely adequate for present needs.

The first shape factor — that for elastic bending — is defined as the ratio of the stiffness S_B of the shaped beam to that, S_B^o , of a solid circular section (second moment I^o) with the same cross-section A , and thus the mass per unit length. Using equation (7.1) we find

$$\phi_B^e = \frac{S_B}{S_B^o} = \frac{I}{I^o}$$

Now I^o for a solid circular section of area A (Table 7.1) is just

$$I^o = \pi r^4 = \frac{A^2}{4\pi} \tag{7.3}$$

from which

$$\phi_B^e = \frac{4\pi I}{A^2} \tag{7.4}$$

Note that it is dimensionless — I has dimensions of (length)⁴ and so does A^2 . It depends only on shape: big and small beams have the same value of ϕ_B^e if their section shapes are the same. This is shown in Figure 7.4: the three rectangular wood sections all have the same shape factor ($\phi_B^e = 2$); the three I-sections also have the same shape factor ($\phi_B^e = 10$). In each group the scale changes but the shape does not — each is a magnified or shrunken version of its neighbour. Shape factors ϕ_B^e for common shapes, calculated from the expressions for A and I in Table 7.1, are listed in the first column of Table 7.2. Solid equiaxed sections (circles, squares, hexagons, octagons) all have values very close to 1 — for practical purposes they can be set equal to 1. But if the section is elongated, or hollow, or of I-section, or corrugated, things change: a thin-walled tube or a slender I-beam can have a value of ϕ_B^e of 50 or more. Such a shape is efficient in that it uses less material (and thus

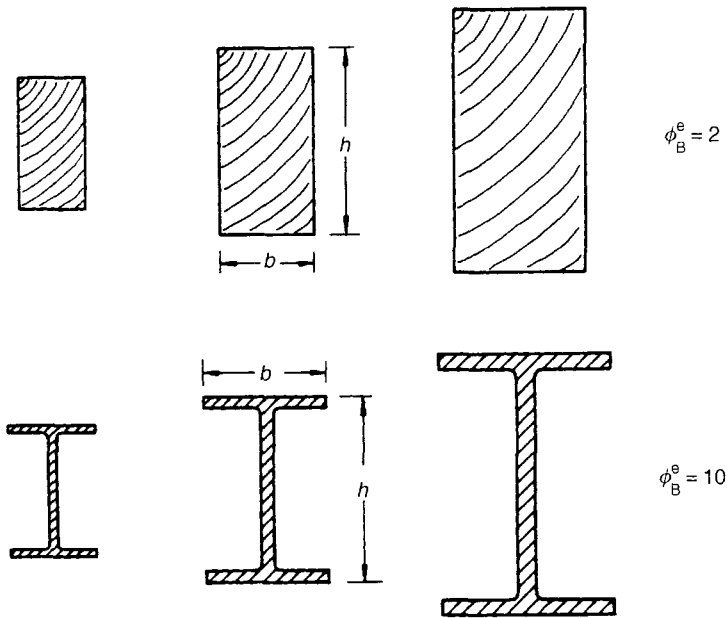


Fig. 7.4 A set of rectangular sections with $\phi_B^e = 2$, and a set of I-sections with $\phi_B^e = 10$. Members of a set differ in size but not in shape.

less mass) to achieve the same bending stiffness*. A beam with $\phi_B^e = 50$ is 50 times stiffer than a solid beam of the same weight.

Shapes which resist bending well may not be so good when twisted. The stiffness of a shaft — the torque T divided by the angle of twist θ (Figure 7.2(c)) — is given by

$$S_T = \frac{KG}{\ell} \quad (7.5)$$

where G is the shear modulus. Shape enters this time through the torsional moment of area, K . For circular sections it is identical with the polar moment of area, J :

$$J = \int_{\text{section}} r^2 dA \quad (7.6)$$

where dA is the differential element of area at the radial distance r , measured from the centre of the section. For non-circular sections, K is less than J ; it is defined (Young, 1989) such that the angle of twist θ is related to the torque T by

$$\theta = \frac{T\ell}{KG} \quad (7.7)$$

where ℓ is length of the shaft and G the shear modulus of the material of which it is made. Approximate expressions for K are listed in Table 7.1.

* This shape factor is related to the radius of gyration, R_g , by $\phi_B^e = 4\pi R_g^2/A$. It is related to the 'shape parameter', k_1 , of Shanley (1960) by $\phi_B^e = 4\pi k_1$. Finally, it is related to the 'aspect ratio' α and 'sparsity ratio' i of Parkhouse (1984, 1987) by $\phi_B^e = i\alpha$.

The shape factor for elastic twisting is defined, as before, by the ratio of the torsional stiffness of the shaped section, S_T , to that, S_T^o , of a solid circular shaft of the same length ℓ and cross-section A , which, using equation (7.5), is

$$\phi_T^e = \frac{S_T}{S_T^o} = \frac{K}{K^o}$$

The torsional constant K^o for a solid cylinder (Table 7.1) is

$$K^o = \frac{\pi}{2} r^4 = \frac{A^2}{2\pi}$$

giving

$$\phi_T^e = \frac{2\pi K}{A^2}$$

(7.8)

It, too, has the value 1 for a solid circular cylinder, and values near 1 for any solid, equiaxed section; but for thin-walled shapes, particularly tubes, it can be large. As before, sets of sections with the same value of ϕ_T^e differ in size but not shape. Values, derived from the expressions for K and A in Table 7.1, are listed in Table 7.2.

Failure in bending and twisting*

Plasticity starts when the stress, somewhere, first reaches the yield strength, σ_y ; fracture occurs when this stress first exceeds the fracture strength, σ_f ; fatigue failure if it exceeds the endurance limit σ_e . Any one of these constitutes failure. As in earlier chapters, we use the symbol σ_f for the failure stress, meaning 'the local stress which will first cause yielding or fracture or fatigue failure.' One shape factor covers all three.

In bending, the stress is largest at the point y_m in the surface of the beam which lies furthest from the neutral axis; it is:

$$\sigma = \frac{M y_m}{I} = \frac{M}{Z} \tag{7.9}$$

where M is the bending moment. Thus, in problems of failure of beams, shape enters through the section modulus, $Z = I/y_m$. If this stress exceeds σ_f the beam will fail, giving the failure moment

$$M_f = Z\sigma_f \tag{7.10}$$

The shape factor for failure in bending, ϕ_B^f , is defined as the ratio of the failure moment M_f (or equivalent failure load F_f) of the shaped section to that of a solid circular section with the same cross-sectional area A :

$$\phi_B^f = \frac{M_f}{M_f^o} = \frac{Z}{Z^o}$$

The quantity Z^o for the solid cylinder (Table 7.1) is

$$Z^o = \frac{\pi}{4} r^3 = \frac{A^{3/2}}{4\sqrt{\pi}}$$

* The definitions of ϕ_B^f and of ϕ_T^f differ from those in the first edition of this book; each is the square root of the old one. The new definitions allow simplification.

giving

$$\phi_B^f = \frac{4\sqrt{\pi}Z}{A^{3/2}} \quad (7.11)$$

Like the other shape factors, it is dimensionless, and therefore independent of scale; and its value for a beam with a solid circular section is 1. Table 7.2 gives expressions for other shapes, derived from the values of the section modulus Z which can be found in Table 7.1.

In torsion, the problem is more complicated. For circular tubes or cylinders subjected to a torque T (as in Figure 7.2c) the shear stress τ is a maximum at the outer surface, at the radial distance r_m from the axis of bending:

$$\tau = \frac{Tr_m}{J} \quad (7.12)$$

The quantity J/r_m in twisting has the same character as $Z = I/y_m$ in bending. For non-circular sections with ends that are free to warp, the maximum surface stress is given instead by

$$\tau = \frac{T}{Q} \quad (7.13)$$

where Q , with units of m^3 , now plays the role of J/r_m or Z (details in Young, 1989). This allows the definition of a shape factor, ϕ_T^f for failure in torsion, following the same pattern as before:

$$\phi_T^f = \frac{T_f}{T_f^o} = \frac{Q}{Q^o} = \frac{2\sqrt{\pi}Q}{A^{3/2}} \quad (7.14)$$

Values of Q and ϕ_T^f are listed in Tables 7.1 and 7.2. Shafts with solid equiaxed sections all have values of ϕ_T^f close to 1.

Fully plastic bending or twisting (such that the yield strength is exceeded throughout the section) involve a further pair of shape factors. But, generally speaking, shapes which resist the onset of plasticity well are resistant to full plasticity also. New shape factors for these are not, at this stage, necessary.

Axial loading and column buckling

A column, loaded in compression, buckles elastically when the load exceeds the Euler load

$$F_c = \frac{n^2\pi^2E I_{\min}}{\ell^2} \quad (7.15)$$

where n is a constant which depends on the end-constraints. The resistance to buckling, then, depends on the smallest second moment of area, I_{\min} , and the appropriate shape factor (ϕ_B^e) is the same as that for elastic bending (equation (7.4)) with I replaced by I_{\min} .

A beam or shaft with an elastic shape factor of 50 is 50 times stiffer than a solid circular section of the same mass per unit length; one with a failure shape factor of 20 is 20 times stronger. If you wish to make stiff, strong structures which are efficient (using as little material as possible) then

making the shape factors as large as possible is the way to do it. It would seem, then, that the bigger the value of ϕ the better. True, but there are limits. We examine them next.

7.3 The efficiency of standard sections

There are practical limits for the thinness of sections, and these determine, for a given material, the maximum attainable efficiency. These limits may be imposed by manufacturing constraints: the difficulty or expense of making an efficient shape may simply be too great. More often they are imposed by the properties of the material itself because these determine the failure mode of the section. Here we explore the ultimate limits for shape efficiency. This we do in two ways. The first (this section) is empirical: by examining the shapes in which real materials — steel, aluminium, etc. — are actually made, recording the limiting efficiency of available sections. The second is by the analysis of the mechanical stability of shaped sections, explored in the following section.

Standard sections for beams, shafts, and columns are generally *prismatic*; prismatic shapes are easily made by rolling, extrusion, drawing, pultrusion or sawing. Figure 7.5 shows the taxonomy of the kingdom of prismatic shapes. The section may be solid, closed-hollow (like a tube or box) or open-hollow (an I-, U- or L-section, for instance). Each class of shape can be made in a range of materials. Those for which standard, off-the-shelf, sections are available are listed on the figure: steel, aluminium, GFRP and wood. Each section has a set of *attributes*: they are the parameters used in structural or mechanical design. They include its dimensions and its section properties (the ‘moments’ I , K and the ‘section moduli’ Z and Q) defined in the previous section.

These are what we need to allow the limits of shape to be explored. Figures 7.6 show I , K , Z and Q plotted against A , on logarithmic scales for standard steel sections. Consider the first, Figure 7.6(a). It shows $\log(I)$ plotted against $\log(A)$. Taking logarithms of the equation for the first shape factor ($\phi_B^e = 4\pi I/A^2$) gives, after rearrangement,

$$\log I = 2 \log A + \log \frac{\phi_B^e}{4\pi}$$

meaning that values of ϕ_B^e appear as a family of parallel lines, all with slope 2, on the figure. The data are bracketed by the values $\phi_B^e = 1$ (solid circular sections) and $\phi_B^e = 65$, the *empirical upper limit* for the shape factor characterizing stiffness in bending for simple structural steel sections. An analogous construction for torsional stiffness (involving $\phi_T^e = 2\pi K/A^2$), shown in Figure 7.6(b), gives a measure of the upper limits for this shape factor; they are listed in the first row of Table 7.3. Here the closed sections group into the upper band of high ϕ_T^e ; the open sections group into a band with a much lower ϕ_T^e because they have poor torsional stiffness, and shape factors which are less than 1.

The shape factors for strength are explored in a similar way. Taking logs of that for failure in bending (using $\phi_B^f = 4\sqrt{\pi}Z/A^{3/2}$) gives

$$\log Z = \frac{3}{2} \log A + \log \frac{\phi_B^f}{4\sqrt{\pi}}$$

Values of ϕ_B^f appear as lines of slope 3/2 on Figure 7.6(c), which shows that, for steel, real sections have values of this shape factor with an upper limit of about 13. The analogous construction for torsion (using $\phi_T^f = 2\sqrt{\pi}Q/A^{3/2}$), shown in Figure 7.6(d), gives the results at the end of the first row of Table 7.3. Here, again, the open sections cluster in a lower band than the closed ones because they are poor in torsion.

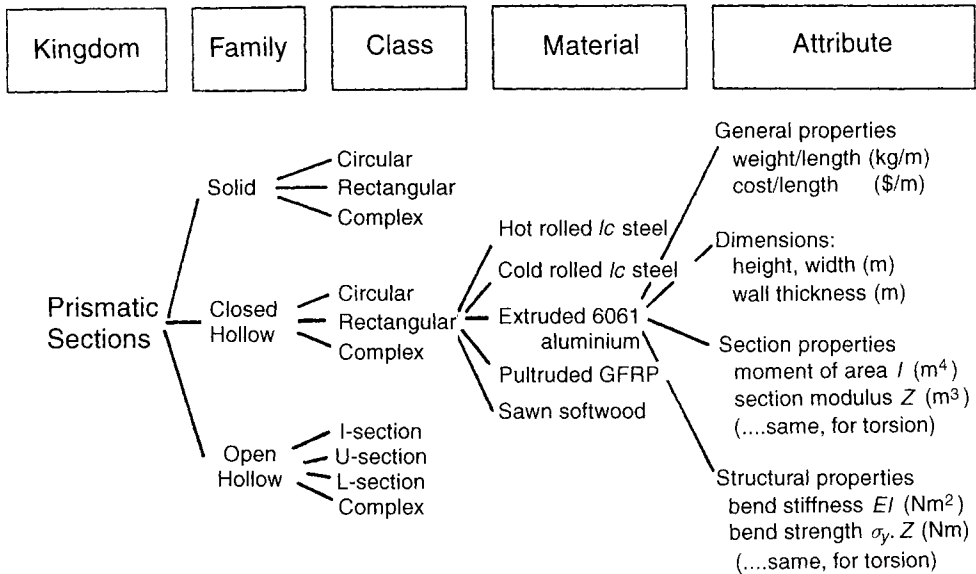


Fig. 7.5 A taxonomy of prismatic shapes, illustrating the attributes of a shaped section.

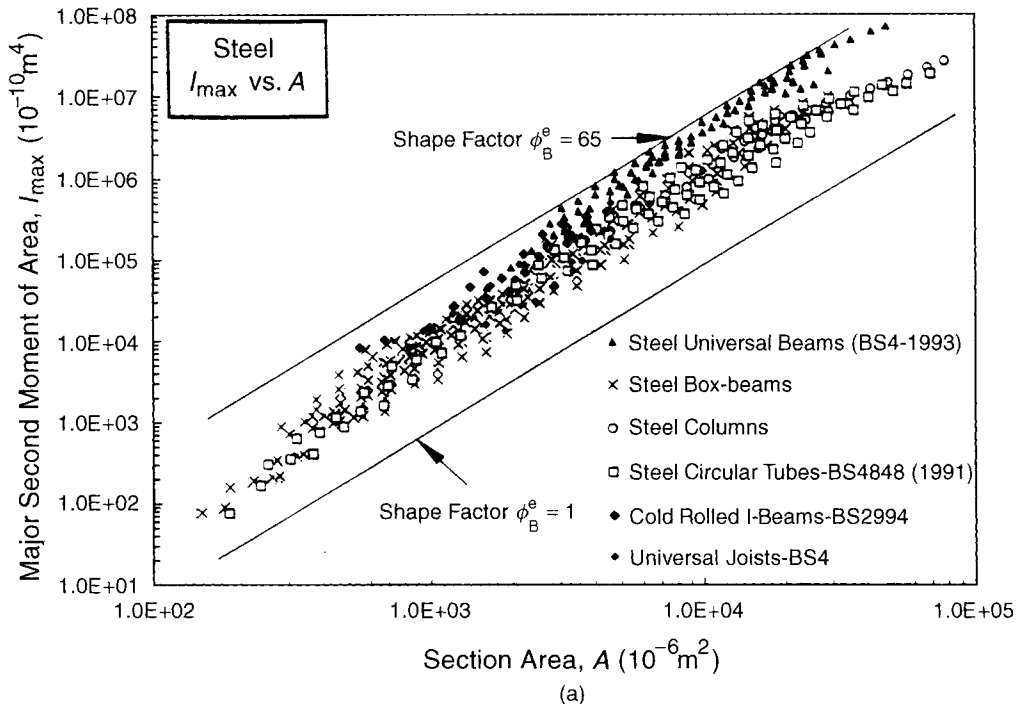


Fig. 7.6 Empirical upper limits for shape factors for steel sections: (a) $\log(I)$ plotted against $\log(A)$; (b) $\log(Z)$ plotted against $\log(A)$; (c) $\log(K)$ plotted against $\log(A)$; (d) $\log(Q)$ plotted against $\log(A)$.

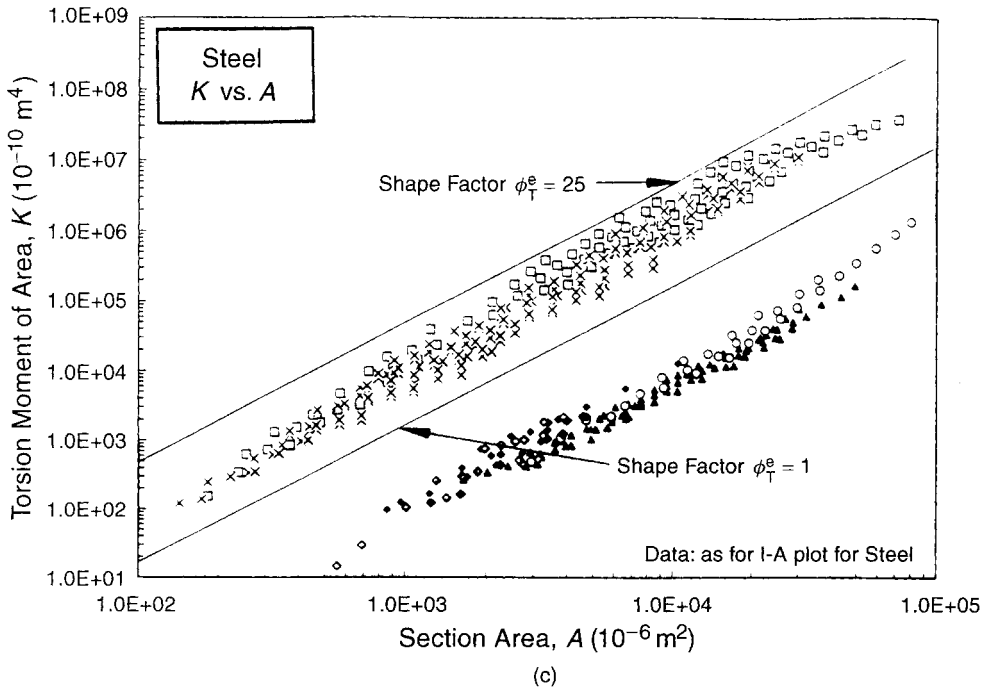
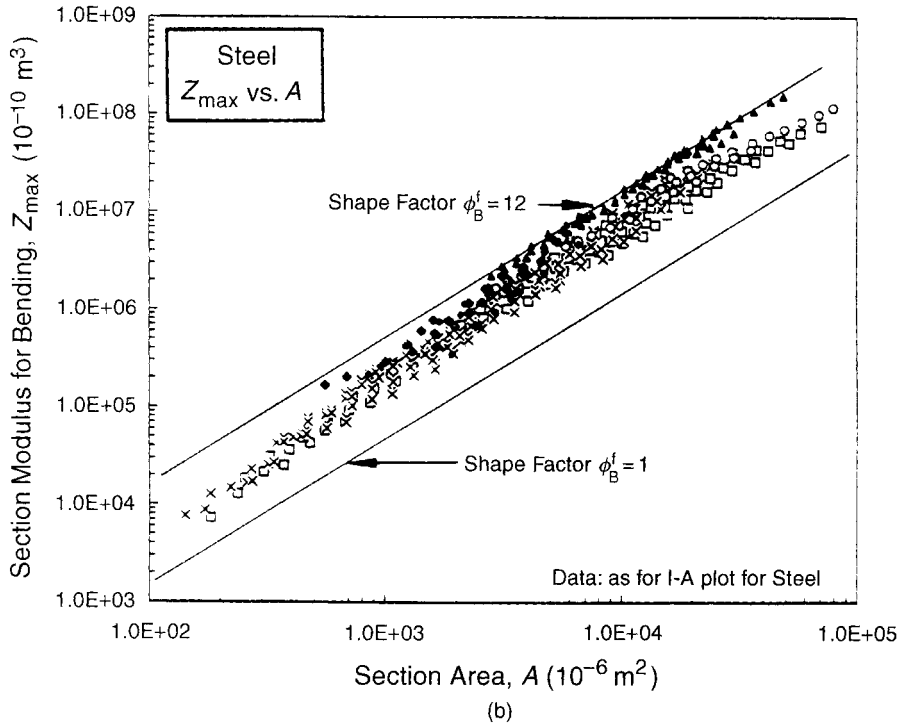


Fig. 7.6 (continued)

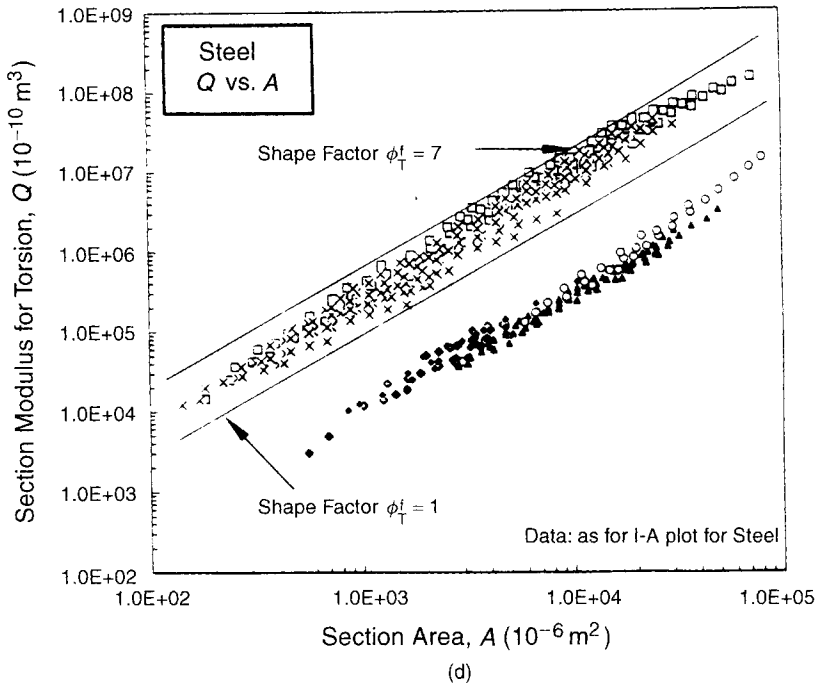


Fig. 7.6 (continued)

Table 7.3 Upper limits for the shape factors ϕ_B^e , ϕ_T^e , ϕ_B^f and ϕ_T^f

Material	$(\phi_B^e)_{\max}$	$(\phi_T^e)_{\max}$	$(\phi_B^f)_{\max}$	$(\phi_T^f)_{\max}$
Structural steels	65	25	13	7
Aluminium alloys	44	31	10	8
GFRP and CFRP	39	26	9	7
Polymers (e.g. nylons)	12	8	5	4
Woods (solid sections)	5	1	3	1
Elastomers	<6	3	—	—

Similar plots for extruded aluminium, pultruded GFRP, wood, nylon and rubber give the results shown in the other rows of the table. It is clear that the *upper-limiting shape factor for simple shapes depends on material*.

The upper limits for shape efficiency are important. They are central to the design of lightweight structures, and structures in which, for other reasons (cost, perhaps) the material content should be minimized. Three questions then arise. What sets the upper limit on shape efficiency of Table 7.3? Why does the limit depend on material? And what, in a given application where efficiency is sought, is the best combination of material and shape? We address these questions in turn.

7.4 Material limits for shape factors

The range of shape factor for a given material is limited either by manufacturing constraints, or by local buckling. Steel, for example, can be drawn to thin-walled tubes or formed (by rolling, folding

or welding) into efficient I-sections; shape factors as high as 50 are common. Wood cannot so easily be shaped; ply-wood technology could, in principle, be used to make thin tubes or I-sections, but in practice, shapes with values of ϕ greater than 5 are uncommon. That is a manufacturing constraint. Composites, too, can be limited by the present difficulty in making them into thin-walled shapes, although the technology for doing this now exists.

When efficient shapes *can* be fabricated, the limits of the efficiency derive from the competition between failure modes. Inefficient sections fail in a simple way: they yield, they fracture, or they suffer large-scale buckling. In seeking efficiency, a shape is chosen which raises the load required for the simple failure modes, but in doing so the structure is pushed nearer the load at which other modes — particularly those involving local buckling — become dominant. It is a characteristic of shapes which approach their limiting efficiency that two or more failure modes occur at almost the same load.

Why? Here is a simple-minded explanation. If failure by one mechanism occurs at a lower load than all others, the section shape can be adjusted to suppress it; but this pushes the load upwards until another mechanism becomes dominant. If the shape is described by a single variable (ϕ) then when two mechanisms occur at the same load you have to stop — no further shape adjustment can improve things. Adding webs, ribs or other stiffeners, gives further variables, allowing shape to be optimized further, but we shall not pursue that here.

The best way to illustrate this is with an example. We take that of a tubular column. The column (Figure 7.7) is progressively loaded in compression. If sufficiently long and thin, it will first fail by general *elastic (Euler) buckling*. The buckling load is increased with no change in mass if the diameter of the tube is increased and the wall thickness correspondingly reduced. But there is a limit to how far this can go because new failure modes appear: if the load rises too far, the tube will *yield plastically*, and if the tube wall is made too thin, it will fail by *local buckling*. Thus there are three competing failure modes: general buckling, local buckling (both influenced by the modulus of the material and the section shape) and plastic collapse (dependent on the yield strength of the material and — for axial loading — dependent on the area of the cross-section but not on its shape). The most efficient shape for a given material is the one which, for a given load, uses the least material. It is derived as follows.

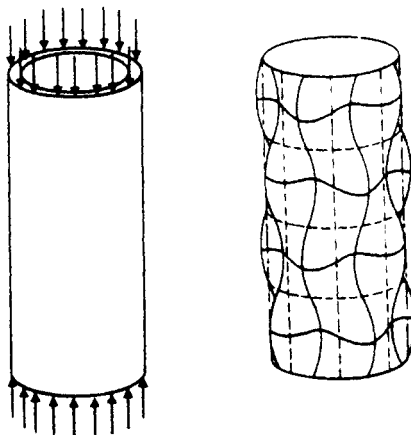


Fig. 7.7 A tube loaded in compression. The upper limit on shape is determined by a balance between failure mechanisms, of which one — local ('chessboard') buckling — is shown in the right-hand figure.

General buckling of a column of height ℓ , radius r , wall thickness t and cross-sectional area $A = 2\pi r t$ with ends which are free to rotate, occurs at the load

$$F = \frac{\pi^2 EI}{\ell^2} \quad (7.16)$$

where, for thin-walled tubes, $I = \pi r^3 t$, and E is the value of Young's modulus for the material of which the column is made. Dividing equation (7.16) by A^2 , substituting for I/A^2 from

$$\phi = \frac{4\pi I}{A^2} = \frac{r}{t} \quad (7.17)$$

where we use the short-hand ϕ for ϕ_B^e . Writing $F/A = \sigma$ where σ is the axial stress in the tube wall, we obtain an expression for the value of the stress σ_1 at the onset of general buckling:

$$(mechanism 1) \quad \sigma_1 = \left(\frac{\pi}{4} E \phi \frac{F}{\ell^2} \right)^{1/2} \quad (7.18)$$

Local buckling is characterized by the 'chessboard' pattern of Figure 7.7. This second failure mode occurs in a thin-walled tube when the axial stress exceeds, approximately, the value (Young, 1989, p. 262–263)

$$(mechanism 2) \quad \sigma_2 = 0.6\alpha E \frac{t}{r} = 0.6\alpha \frac{E}{\phi} \quad (7.19)$$

(using equation (7.17) to introduce ϕ). This expression contains an empirical knockdown factor, α , which Young (1989) takes to equal 0.5 to allow for the interaction of different buckling modes.

The final failure mode is that of general yield. It occurs when the wall-stress exceeds the value

$$(mechanism 3) \quad \sigma_3 = \sigma_y \quad (7.20)$$

where σ_y is the yield strength of the material of the tube.

We now have the stresses at which each failure mechanism first occurs. The one which is dominant is the one that cuts in first — that is, it has the lowest failure stress. Mechanism 1 is dominant when the value of σ_1 is lower than either σ_2 or σ_3 , mechanism 2 when σ_2 is the least, and so on. The boundaries between the three fields of dominance are found by equating the equations for σ_1 , σ_2 and σ_3 (equations (7.18), (7.19) and (7.20)) taken in pairs, giving

$$(1-2 \text{ boundary}) \quad \frac{F}{\sigma_y \ell^2} = \frac{1.44\alpha^2}{\pi} \left(\frac{E}{\sigma_y} \right) \frac{1}{\phi^3} \quad (7.21a)$$

$$(1-3 \text{ boundary}) \quad \frac{F}{\sigma_y \ell^2} = \frac{4}{\pi} \left(\frac{\sigma_y}{E} \right) \frac{1}{\phi} \quad (7.21b)$$

$$(2-3 \text{ boundary}) \quad \phi = 0.6\alpha \left(\frac{E}{\sigma_y} \right) \quad (7.21c)$$

Here we have arranged the variables into dimensionless groups. There are just three: the first is the *load factor* $F/\sigma_y \ell^2$, the second is the *yield strain* σ_y/E and the last is the *shape factor* ϕ . This allows a simple presentation of the failure-mechanism boundaries, and the associated fields of dominance, as shown in Figure 7.8. The axes are the load factor $F/\sigma_y \ell^2$ and the shape factor ϕ . The diagram is constructed for a specific value of the yield strain σ_y/E of 3×10^{-3} . Changing σ_y/E moves the boundaries a little, but leaves the general picture unchanged.

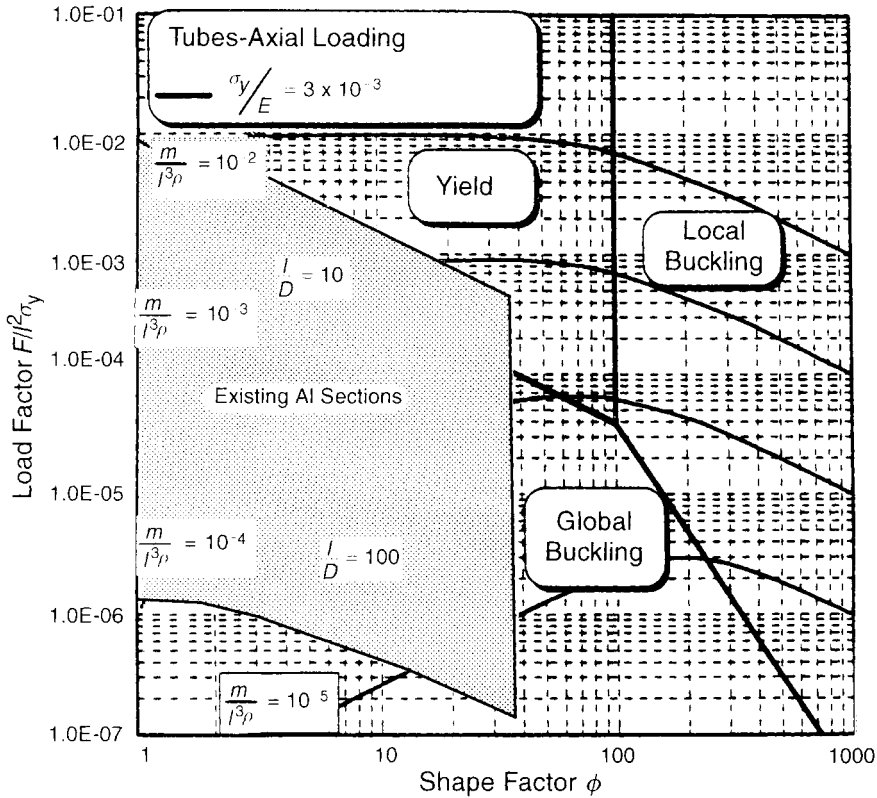


Fig. 7.8 A plot of the load factor $F/\sigma_y \ell^2$ against shape factor ϕ for $\sigma_y/E = 3 \times 10^{-3}$ for axially loaded tubes. The grey area shows where standard sections lie. The upper limit falls just below the boundary between yield and local buckling.

To explore *efficiency* we need one more step. According to the simple-minded argument, above, maximum efficiency is found when two failure modes occur at the same load. Let us be more precise, and see whether simple-mindedness is justified. To do this we calculate the mass of the column which will just not fail by any one of the mechanisms, and then seek a way of minimizing this with respect to ϕ . The mass, m , of the column is

$$m = A \ell \rho \quad (7.22)$$

where A is the area of its cross-section and ρ is the density of the material of which it is made. Within the general-buckling regime 1, the minimum section area A which will just support F is

$$A_1 = \frac{F}{\sigma_1}$$

Inserting this into equation (7.22) and replacing σ_1 by equation (7.18) gives for regime 1:

$$(\text{mass in regime 1}) \left(\frac{m}{\ell^3 \rho} \right) = \left(\frac{4}{\pi} \left(\frac{1}{\phi} \right) \left(\frac{F}{\sigma_y \ell^2} \right) \left(\frac{\sigma_y}{E} \right) \right)^{1/2} \quad (7.23a)$$

Within the local buckling regime 2, equation (7.19) for σ_2 dominates and we find instead

$$(\text{mass in regime 2}) \quad \left(\frac{m}{\ell^3 \rho} \right) = \left(\frac{\phi}{0.6\alpha} \right) \left(\frac{F}{\sigma_y \ell^2} \right) \left(\frac{\sigma_y}{E} \right) \quad (7.23b)$$

and for the yield regime 3, using equation (7.20) for σ_3 :

$$(\text{mass in regime 3}) \quad \left(\frac{m}{\ell^3 \rho} \right) = \left(\frac{F}{\sigma_y \ell^2} \right) \quad (7.23c)$$

As before, the variables have been assembled into dimensionless groups; there is one new one: the mass is described by the group $(m/\ell^3 \rho)$. For a chosen value of this quantity and of the yield strain σ_y/E , each equation becomes a relation between the load factor, $F/\sigma_y \ell^2$, and the shape factor, ϕ , allowing contours of mass to be plotted on the diagram, as shown in Figure 7.8.

We can now approach the question: what is the most efficient shape, measured by ϕ , for the cross-section of the column? Tracking across Figure 7.8 from left to right at a given value of the load factor, the mass at first falls and then rises again. In the lower half of the diagram the minimum mass lies at or near the 1–2 boundary; higher up it lies slightly to the left of the 2–3 boundary. So, like all good simple-minded explanations, this one is almost right — right enough to be useful.

If the column is designed for a *specific* value of the load factor, the optimum ϕ can be read from the diagram. But if the column is intended as a *general-purpose component*, the load factor is not known, though all reasonable values lie well within the range shown in the vertical axis of Figure 7.8. Then the safest choice is a value of ϕ a little to the left of the 2–3 (yield-local buckling) boundary, since this ensures that, if the column were to fail, it would fail by yield rather than the more catastrophic local buckling. This boundary lies at the position given by equation (7.21c). Allowing a margin of reserve of 1.5 (by reducing ϕ by a factor of 2/3) we find the optimal shape factor for the tubular column to be

$$\phi_{\text{opt}} = \left(\frac{r}{t} \right)_{\text{opt}} \approx 0.4\alpha \frac{E}{\sigma_y}$$

which for $\alpha = 0.5$ is

$$\phi_{\text{opt}} = \left(\frac{r}{t} \right)_{\text{opt}} \approx 0.2 \frac{E}{\sigma_y} \quad (7.24)$$

This is a single example of how competing failure mechanisms determine shape efficiencies. Other modes of loading (bending, torsion) and other classes of shape (box-sections, I-sections) each require analysis, and this is a painfully tedious process, best left to others. Others have done it* and find that all combinations of loading and shape lead to diagrams which resemble Figure 7.8. The limiting efficiency depends to some extent on details of loading and class of shape, but not much. The broad conclusion: the ultimate limit for simple shapes (tubes, box-sections, I-sections) is set by material properties, and is approximated by equation (7.4).

Much higher efficiencies are possible when precise loading conditions are known, allowing customized application of stiffeners and webs to suppress local buckling. This allows a further increase in the ϕ s until failure or new, localized, buckling modes appear. These, too, can be suppressed by a further hierarchy of structuring; ultimately, the ϕ s are limited only by manufacturing constraints. But for a general selection of material and shape, this is getting too sophisticated, and equation (7.24) above is the best approximation.

* See, for example, the Weaver and Ashby (1998).

7.5 Material indices which include shape

The performance-maximizing combination of material and section shape, for a given mode of loading, is found as follows. The method follows that of Chapter 5, with one extra step to bring in the shape.

Axial tension of ties

The ability of a tie to carry a load F without deflecting excessively or failing depends only on the area of its section, but not on its shape. The material index for stiffness at minimum weight, E/ρ , holds for all section shapes. This, as we have said, is not true of bending or twisting, or when columns buckle.

Elastic bending of beams and twisting of shafts

Consider the selection of a material for a beam of specified stiffness S_B and length ℓ , and it is to have minimum mass, m . The selection must allow for the fact that the available candidate-materials have section shapes which differ. The mass m of a beam of length ℓ and section area A is given by equation (7.22). Its bending stiffness is given by equation (7.1). Replacing I by ϕ_B^e using equation (7.4) gives

$$S_B = \frac{C_1 E}{4\pi \ell^3} \phi_B^e A^2 \quad (7.25)$$

Using this to eliminate A in equation (7.25) gives the mass of the beam:

$$m = \left[\frac{4\pi S_B}{C_1 \ell} \right]^{1/2} \ell^3 \left[\frac{\rho^2}{\phi_B^e E} \right]^{1/2} \quad (7.26)$$

For beams with the same shape, for which ϕ_B^e is constant, the best choice for the lightest beam is the material with the greatest value of $E^{1/2}/\rho$ — the result derived in Chapter 5 (note that this applies to material selection for all self-similar shapes, not just solid ones). But if we wish to select a material–shape combination for a light stiff beam, the best choice is that with the greatest value of the index

$$M_1 = \frac{[E\phi_B^e]^{1/2}}{\rho} \quad (7.27)$$

Exactly the same result holds for the general elastic buckling of an axially loaded column.

The procedure for elastic twisting of shafts is similar. A shaft of section A and length ℓ is subjected to a torque T . It twists through an angle θ . It is required that the torsional stiffness, T/θ , meet a specified target S_T , at minimum mass. The mass of the shaft is given, as before, by equation (7.24). Its torsional stiffness is

$$S_T = \frac{KG}{\ell}$$

where G is the shear modulus, and K was defined earlier. Replacing K by ϕ_T^e using equation (7.8) gives

$$S_T = \frac{G}{2\pi\ell} \phi_T^e A^2 \quad (7.28)$$

Using this to eliminate A in equation (7.24) gives

$$m = \left[2\pi \frac{S_T}{\ell^3} \right]^{1/2} \ell^3 \left[\frac{\rho^2}{\phi_T^e G} \right]^{1/2}$$

The best material-and-shape combination is that with the greatest value of $[\phi_T^e G]^{1/2}/\rho$. The shear modulus, G , is closely related to Young's modulus E . For the practical purposes we approximate G by $3/8E$; then the index becomes

$$M_2 = \frac{[\phi_T^e E]^{1/2}}{\rho} \quad (7.29)$$

For shafts of the same shape, this reduces to $E^{1/2}/\rho$ again. When shafts differ in both material and shape, the material index (7.29) is the one to use.

Failure of beams and shafts

A beam, loaded in bending, must support a specified load F without failing. The mass of the beam is to be minimized. When shape is not a consideration, the best choice (Chapter 5) is that of the material with the greatest value of $\sigma_f^{2/3}/\rho$ where σ_f is the failure strength of the material. When section-shape is a variable, the best choice is found as follows.

Failure occurs if the load exceeds the failure moment

$$M_f = Z\sigma_f$$

Replacing Z by the appropriate shape-factor ϕ_B^f via equation (7.11) gives

$$M_f = \frac{\sigma_f}{4\sqrt{\pi}} \phi_B^f A^{3/2} \quad (7.30)$$

Substituting this into equation (7.22) for the mass of the beam gives

$$m = \left(4\sqrt{\pi} \frac{M_f}{\ell^3} \right)^{2/3} \ell^3 \left[\frac{\rho^{3/2}}{\phi_B^f \sigma_f} \right]^{2/3} \quad (7.31)$$

The best material-and-shape combination is that with the greatest value of the index

$$M_3 = \frac{(\phi_B^f \sigma_f)^{2/3}}{\rho} \quad (7.32)$$

At constant shape the index reduces to the familiar $\sigma_f^{2/3}/\rho$ of Chapter 5; but when shape as well as material can be chosen, the full index must be used.

The twisting of shafts is treated in the same way. A shaft must carry a torque T without failing. This requires that T not exceed the failure torque T_f , where, from equation (7.13),

$$T_f = Q\tau_f$$

Replacing Q by ϕ_T^f with equation (7.14) gives

$$T_f = \frac{\sigma_f}{4\sqrt{\pi}} \phi_T^f A^{3/2} \quad (7.33)$$

where τ_f , the shear-failure strength has been replaced by $\sigma_f/2$, the tensile failure strength. Using this to eliminate the area A in equation (7.34) for the mass of the shaft gives

$$m = \left(4\sqrt{\pi} \frac{T_f}{\ell^3}\right)^{2/3} \ell^3 \left[\frac{\rho^{3/2}}{\phi_T^f \sigma_f}\right]^{2/3} \quad (7.34)$$

Performance is maximized by the selection which has the greatest value of

$$M_4 = \frac{(\phi_T^f \sigma_f)^{2/3}}{\rho} \quad (7.35)$$

Constrained shapes

The geometry of a design sometimes imposes constraints on shape. Panels, for example, usually have a fixed width but a thickness which is ‘free’, meaning that it can be chosen to give a desired bending stiffness; the shape of the section, too, is free: it could, for example, be a honeycomb. Beams, too, may be constrained in either height or width. When there is a dimensional constraint, the definition of the shape factor changes. Material indices for constrained shapes are discussed in the Appendix to this chapter.

7.6 The microscopic or micro-structural shape factor

Microscopic shape

The sections listed in Tables 7.1 and 7.2 achieve efficiency through their *macroscopic* shape. Efficiency can be achieved in another way: through shape on a small scale; *microscopic* or ‘micro-structural’ shape. Wood is an example. The solid component of wood (a composite of cellulose, lignin and other polymers) is shaped into little prismatic cells, dispersing the solid further from the axis of bending or twisting of the branch or trunk of the tree. This gives wood a greater bending and torsional stiffness than the solid of which it is made. The added efficiency (Figure 7.9) is characterized by a set of *microscopic shape factors*, ψ , with definitions and characteristics exactly like those of ϕ . The characteristic of microscopic shape is that the structure repeats itself: it is *extensive*. The micro-structured solid can be thought of as a ‘material’ in its own right: it has a modulus, a density, a strength, and so forth. Shapes can be cut from it which — provided they are large compared with the size of the cells — inherit its properties. It is possible, for instance, to fabricate an I-section out of wood, and such a section has macroscopic shape (as defined earlier) as well as microscopic shape (Figure 7.10). It is shown in a moment that the total shape factor for a wooden I-beam is the product of the shape factor for the wood structure and that for the I-beam; and this can be large.

Many natural materials have microscopic shape. Wood is just one example. Bone, stalk and cuttle all have structures which give high stiffness at low weight. It is harder to think of man-made examples, although it would appear possible to make them. Figure 7.11 shows four extensive

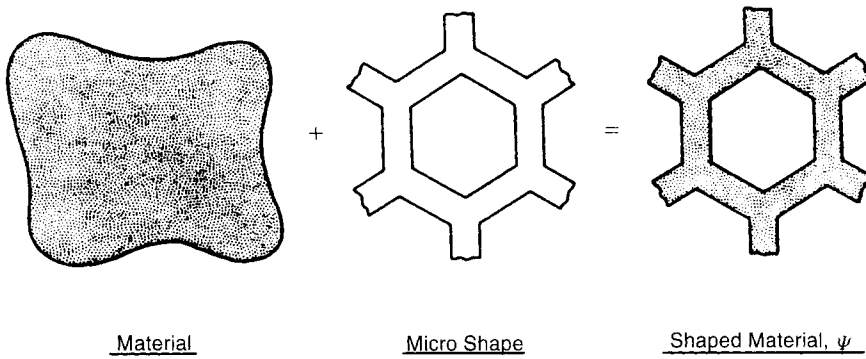


Fig. 7.9 Mechanical efficiency can be obtained by combining material with microscopic, or internal, shape, which repeats itself to give an extensive structure. The shape is characterized by microscopic shape factors, ψ .

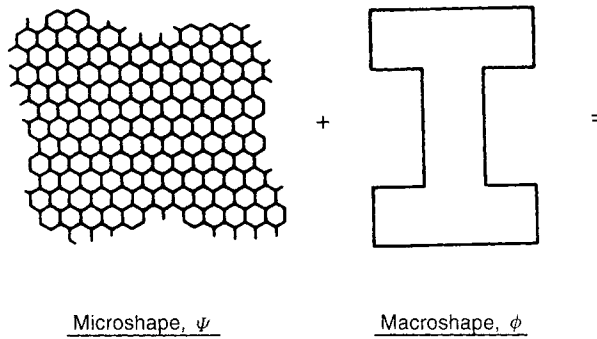


Fig. 7.10 Micro-structural shape can be combined with macroscopic shape to give efficient structures. The schematic is suggested by Parkhouse (1984). The overall shape factor is the product of the microscopic and macroscopic shape factors.

structures with microscopic shape, all of which are found in nature. The first is a wood-like structure of hexagonal-prismatic cells; it has translational symmetry and is uniform, with isotropic properties in the plane of the section when the cells are regular hexagons. The second is an array of fibres separated by a foamed matrix typical of palm wood; it too is uniform in-plane and has translational symmetry. The third is an axisymmetric structure of concentric cylindrical shells separated by a foamed matrix, like the stem of some plants. And the fourth is a layered structure, a sort of multiple sandwich-panel, like the shell of the cuttle fish; it has orthotropic symmetry.

Microscopic shape factors

Consider the gain in bending stiffness when a solid cylindrical beam like that shown as a black circle in Figure 7.11 is expanded, at constant mass, to a circular beam with any one of the structures which surround it in the figure. The stiffness S_s of the original solid beam is

$$S_s = \frac{C_1 E_s I_s}{\ell^3} \quad (7.36)$$

Micro-Structured Materials

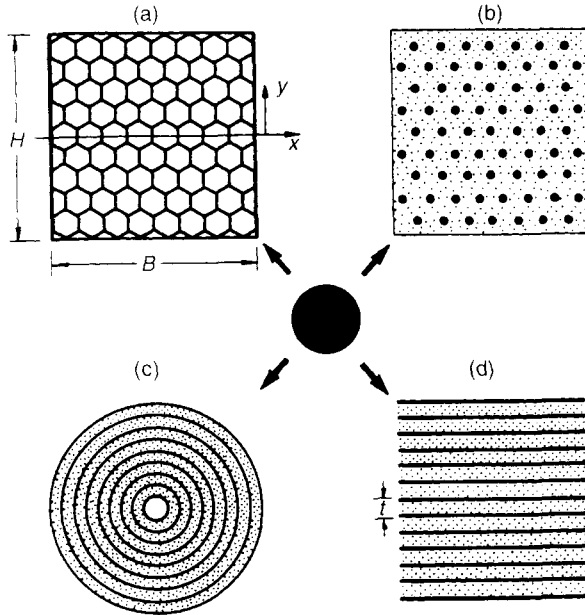


Fig. 7.11 Four extensive micro-structured materials which are mechanically efficient: (a) prismatic cells; (b) fibres embedded in a foamed matrix; (c) concentric cylindrical shells with foam between; and (d) parallel plates separated by foamed spacers.

where the subscript s means a property of the solid beam. When the beam is expanded at constant mass its density falls from ρ_s to ρ and its radius increases from r_s to

$$r = \left(\frac{\rho_s}{\rho} \right)^{1/2} r_s \quad (7.37)$$

with the result that its second moment of area increases from I_s to

$$I = \frac{\pi}{4} r^4 = \frac{\pi}{4} \left(\frac{\rho_s}{\rho} \right)^2 r_s^4 = \left(\frac{\rho_s}{\rho} \right)^2 I_s \quad (7.38)$$

If the cells, fibres, rings or plates in Figure 7.11 are extensive parallel to the axis of the beam, the modulus falls from that of the solid, E_s , to

$$E = \left(\frac{\rho}{\rho_s} \right) E_s \quad (7.39)$$

The stiffness of the expanded beam is thus

$$S = \frac{C_1 EI}{\ell^3} = \frac{C_1 E_s I_s}{\ell^3} \left(\frac{\rho_s}{\rho} \right) \quad (7.40)$$

The microscopic shape factor, ψ is defined in the same way as the macroscopic one, ϕ : it is the ratio of the stiffness of the structured beam to that of the solid one. Taking the ratio of equations (7.40) and (7.36) gives

$$\psi_B^e = \frac{S}{S_s} = \frac{\rho_s}{\rho} \quad (7.41)$$

In words: the microscopic shape factor for prismatic structures is simply the reciprocal of the relative density. Note that, in the limit of a solid (when $\rho^* = \rho_s$) ψ_B^e takes the value 1, as it obviously should. A similar analysis for failure in bending gives the shape factor

$$\psi_B^f = \left(\frac{\rho_s}{\rho} \right)^{1/2} \quad (7.42)$$

Torsion, as always, is more difficult. When the structure of Figure 7.11(c), which has circular symmetry, is twisted, its rings act like concentric tubes and for these

$$\psi_T^e = \frac{\rho_s}{\rho} \quad \text{and} \quad \psi_T^f = \left(\frac{\rho_s}{\rho} \right)^{1/2} \quad (7.43)$$

The others have lower torsion stiffness and strength (and thus lower shape factors) for the same reason that I-sections, good in bending, perform poorly in torsion.

Structuring, then, converts a solid with modulus E_s and strength $\sigma_{f,s}$ to a new solid with properties E and σ_f . If this new solid is formed to an efficient macroscopic shape (a tube, say, or an I-section) its bending stiffness, to take an example, increases by a further factor of ϕ_B^e . Then the stiffness of the beam, expressed in terms of that of the solid of which it is made, is

$$S = \psi_B^e \phi_B^e S_s \quad (7.44)$$

that is, the shape factors multiply. The same is true for strength.

This is an example of structural hierarchy and the benefits it brings. It is possible to extend it further: the individual cell walls or layers could, for instance, be structured, giving a third multiplier to the overall shape factor, and these units, too could be structured (Parkhouse, 1984). Nature does this to good effect, but for man-made structures there are difficulties. There is the obvious difficulty of manufacture, imposing economic limits on the levels of structuring. And there is the less obvious one of reliability. If the structure is optimized, then a failure of a member at one level of the structure could trigger failure of the structure as a whole. The more complex the structure, the harder it becomes to ensure the integrity at all levels.

As pointed out earlier, a micro-structured material can be thought of as a new material. It has a density, a strength, a thermal conductivity, and so on; difficulties arise only if the sample size is comparable to the cell size, when 'properties' become size dependent. This means that micro-structured materials can be plotted on the Material Selection Charts — indeed, wood appears on them already — and that all the selection criteria used for solid materials developed in Chapter 5 apply, unchanged, to the micro-structured materials.

7.7 Co-selecting material and shape

Optimizing the choice of material and shape can be done in several ways. Two are illustrated below.

Co-selection by calculation

Consider as an example the selection of a material for a stiff *shaped* beam of minimum mass. Four materials are available, listed in Table 7.4 with their properties and the shapes, characterized by ϕ_B^e , in which they are available (here, the maximum ones). We want the combination with the largest value of the index M_1 of equation (7.27) which, repeated, is

$$M_1 = \frac{(\phi_B^e E)^{1/2}}{\rho}$$

The second last column shows the simple ‘fixed shape’ index $E^{1/2}/\rho$: wood has the greatest value — it is more than twice as stiff as steel for the same weight. But when each material is shaped efficiently (last column) wood has the *lowest* value of M_1 — even steel is better; the aluminium alloy wins, marginally better than GFRP.

Graphical co-selection using material property charts

Shaped materials can be displayed and selected with the Material Selection Charts. The reasoning, for the case of elastic bending, goes like this. The material index for elastic bending (equation (7.27)) can be rewritten as

$$M_1 = \frac{(\phi_B^e E)^{1/2}}{\rho} = \frac{(E/\phi_B^e)^{1/2}}{\rho/\phi_B^e} \quad (7.45)$$

The equation says: a material with modulus E and density ρ , when structured, behaves like a material with modulus

$$E^* = E/\phi_B^e$$

and density

$$\rho^* = \rho/\phi_B^e$$

The E – ρ chart is shown schematically in Figure 7.12. The structured material properties E^* and ρ^* can be plotted onto it. Introducing shape ($\phi_B^e = 10$, for example) moves the material M to the lower left along a line of slope 1, from the position E , ρ to the position $E/10$, $\rho/10$, as shown in the figure. The selection criteria are plotted onto the figure as before: a constant value of the index of $E^{1/2}/\rho$, for instance, plots as a straight line of slope 2; it is shown, for one value of $E^{1/2}/\rho$, as

Table 7.4 The selection of material and shape for a light, stiff, beam

Material	ρ	E	ϕ_{\max}^*	$E^{1/2}$	$(\phi_{\max} E)^{1/2}$
	Mg/m^3	GPa		ρ	ρ
1020 Steel	7.85	205	65	1.8	14.7
6061-T4 A1	2.7	70	44	3.1	20.5
GFRP (isotropic)	1.75	28	39	2.9	19.0
Wood (oak)	0.9	13.5	5	4.1	9.1

* ϕ_{\max} means the maximum permitted value of ϕ from Table 7.3.

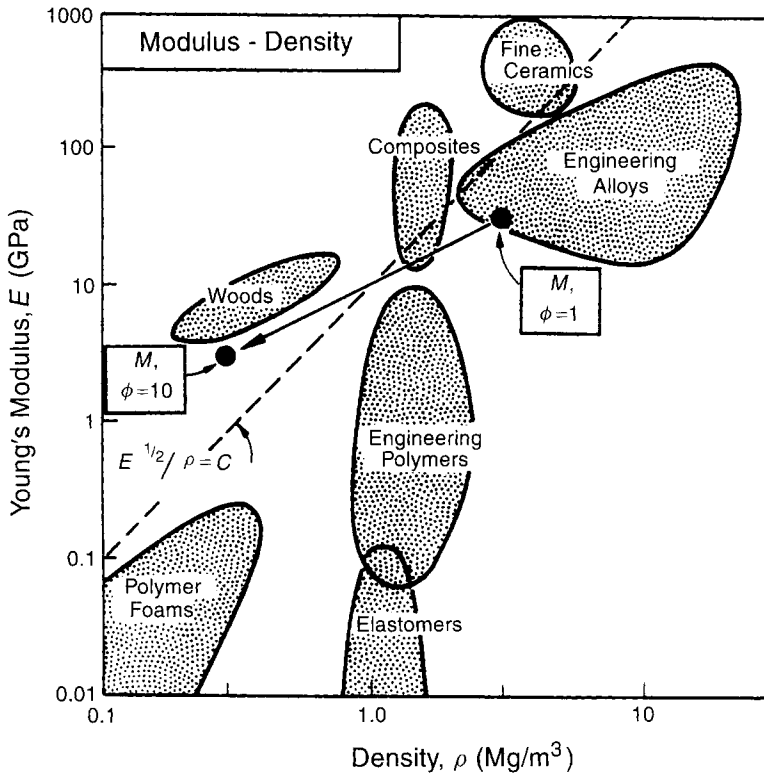


Fig. 7.12 Schematic of Materials Selection Chart 1: Young's modulus plotted against density. The best material-and-shape for a light, stiff beam is that with the greatest value of $E^{1/2}/\rho$. The structured material behaves in bending like a new material with modulus $E^* = E/\phi$ and density $\rho^* = \rho/\phi$ (where ϕ means ϕ_B^e) and can be plotted onto the charts. All the material-selection criteria still apply. A similar procedure is used for torsion.

a broken line. The introduction of shape has moved the material from a position below this line to one above; its performance has improved. Elastic twisting of shafts is treated in the same way.

Materials selection based on strength (rather than stiffness) at a minimum weight uses the chart of strength σ_f against density ρ , shown schematically in Figure 7.13. Shape is introduced in a similar way. The material index for failure in bending (equation (7.32)), can be rewritten as follows

$$M_3 = \frac{(\phi_B^f \sigma_f)^{2/3}}{\rho} = \frac{(\sigma_f / (\phi_B^f)^2)^{2/3}}{\rho / (\phi_B^f)^2} \quad (7.32)$$

The material with strength σ_f and density ρ , when shaped, behaves in bending like a material of strength

$$\sigma_f^* = \sigma_f / (\phi_B^f)^2$$

and density

$$\rho^* = \rho / (\phi_B^f)^2$$

The rest will be obvious. Introducing shape ($\phi_B^f = \sqrt{10}$, say) moves a material M along a line of slope 1, taking it, in the schematic, from a position σ_f, ρ below the material index line (the

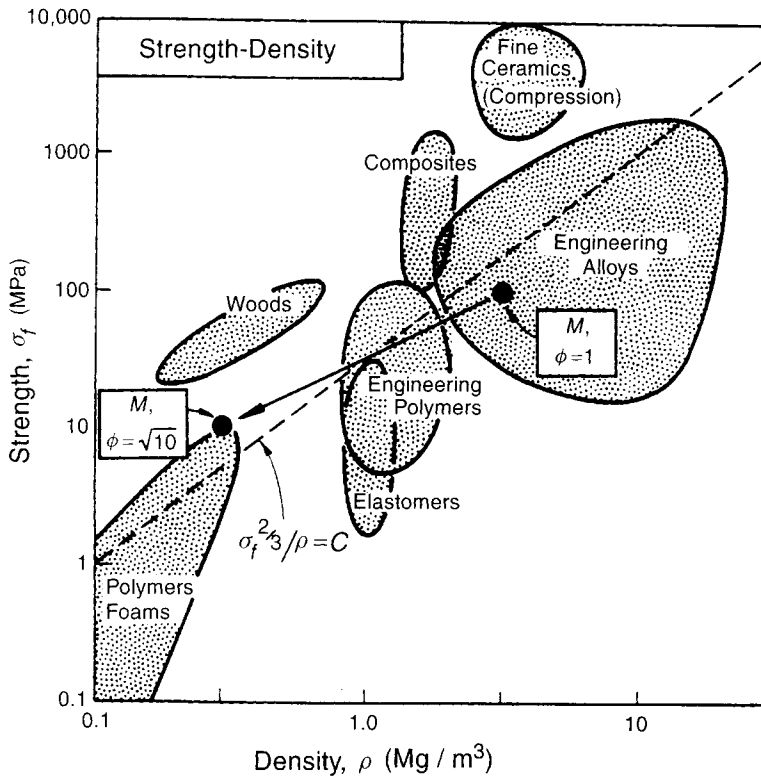


Fig. 7.13 Schematic of Materials Selection Chart 2: strength σ_f plotted against density ρ . The best material for a light, strong beam is that with the greatest value of $\sigma_f^{2/3}/\rho$. The structured material behaves in bending like a new material with strength $\sigma_f^* = \sigma_f/\phi^2$, and density ρ/ϕ^2 (where ϕ means ϕ_B^f), and can be plotted onto the chart. All the material-selection criteria still apply. A similar procedure is used for torsional strength.

broken line) to the position $\sigma_f/10, \rho/10$ which lies above it. The performance has again improved. Torsional failure is analysed by using ϕ_T^f in place of ϕ_B^f .

Examples of the method are given in the case studies of the next chapter.

7.8 Summary and conclusions

The designer has two groups of variables with which to optimize the performance of a load-bearing component: the material properties and the shape of the section. They are not independent. The best choice of material, in a given application, depends on the shapes in which it is available, or to which it could potentially be formed. A procedure is given for simultaneously optimizing the choice of both material and shape.

The contribution of shape is isolated by defining four shape factors. The first, ϕ_B^e , is for the elastic bending and buckling of beams; the second, ϕ_T^e , is for the elastic twisting of shafts; the third, ϕ_B^f

Table 7.5 Definitions of shape factors

<i>Design constraint*</i>	<i>Bending</i>	<i>Torsion</i>
Stiffness	$\phi_B^e = \frac{4\pi I}{A^2}$	$\phi_T^e = \frac{2\pi K}{A^2}$
Strength	$\phi_B^f = \frac{4\sqrt{\pi}Z}{A^{3/2}}$	$\phi_T^f = \frac{2\sqrt{\pi}Q}{A^{3/2}}$

* A = section area; I , K , Z and Q are defined in the text and tabulated in Table 7.1.

is for the plastic failure of beams loading in bending; and the last, ϕ_T^f , is for the plastic failure of twisted shafts (Table 7.5). The shape factors are dimensionless numbers which characterize the efficiency of use of the material in each mode of loading. They are defined such that all four have the value 1 for solid circular sections. With this definition, all equiaxed solid sections have shape factors of about 1, but efficient shapes which disperse the material far from the axis of bending or twisting (I-beams, hollow tubes, sandwich structures, etc.) have large values of the shape factors. They are tabulated for common shapes in Table 7.2.

The best material–shape combination for a light beam with a prescribed bending stiffness is that which maximizes the material index

$$M_1 = \frac{(E\phi_B^e)^{1/2}}{\rho}$$

A similar combination, M_2 , involving ϕ_T^e , gives the lightest stiff shaft. The material–shape combination for a light beam with a prescribed strength is that which maximizes the material index

$$M_3 = \frac{(\phi_B^f \sigma_f)^{2/3}}{\rho}$$

A similar combination, M_4 , involving ϕ_T^f gives the lightest strong shaft. Here, the criterion of ‘performance’ was that of meeting a design specification at minimum weight. Other such material–shape combinations maximize other performance criteria: minimizing cost rather than weight, for example, or maximizing energy storage. Examples are developed in Chapter 8.

The idea of micro-structural shape factors (ψ) is introduced to characterize the efficiency, in bending and torsion, of cellular, layered and other small-scale structures, common in nature. They are defined in the same way as the ϕ s. The difference is that microscopic shape is repeated; structures with microscopic shape are extensive and can themselves be cut to give macroscopic shape as well. Such structures can be thought of either as a solid with properties E_s , $\sigma_{f,s}$ and ρ_s , with a microscopic shape factor of ψ ; or as a new material, with a new set of properties, E_s/ψ , ρ_s/ψ , etc., with a shape-factor of 1. Wood is an example: it can be seen as solid cellulose and lignin shaped to the cells of wood, or as wood itself, with a lower density, modulus and strength than cellulose, but with greater values of indices $E^{1/2}/\rho$ and $\sigma_f^{2/3}/\rho$ which characterize structural efficiency. When micro-structured materials (ψ) are given macroscopic shape (ϕ) the total shape factor is then the product $\phi\psi$, and this can be large.

The procedure for selecting material–shape combinations is best illustrated by examples. These can be found in the next chapter.

7.9 Further reading

Books on the mechanics of materials

Gere, J.M. and Timoshenko, S.P. (1985) *Mechanics of Materials*, Wadsworth International, London.
 Timoshenko, S.P. and Gere, J.M. (1961) *Theory of Elastic Stability*, McGraw-Hill Koga Kusha Ltd, London.
 Young, W.C. (1989) *Roark's Formulas for Stress and Strain*, 6th edition, McGraw-Hill, New York.

Books and articles on the efficiency of structures

Ashby, M.F. (1991) Materials and shape, *Acta Metall. Mater.* **39**, 1025–1039.
 Gerard, G. (1956) *Minimum Weight Analysis of Compression Structures*, New York University Press, New York.
 Parkhouse, J.G. (1984) Structuring: a process of material dilution, in *3rd Int. Conf. on Space Structures*, p. 367, edited by H. Nooshin, Elsevier London.
 Parkhouse, J.G. (1987) Damage accumulation in structures, *Reliability Engineering*, **17**, 97–109.
 Shanley, F.R. (1960) *Weight-Strength Analysis of Aircraft Structures*, 2nd edition, Dover Publications, New York.
 Weaver, P.M. and Ashby, M.F. (1996) The optimal selection of material and section shape, *Journal of Engineering Design*, **7**, 129–150.
 Weaver, P.M. and Ashby, M.F. (1998) Material limits for shape efficiency, *Prog. Mater. Sci.*, **41**, 61–128.

Appendix: geometric constraints and associated shape factors

Geometric constraints

Whenever a free variable is adjusted to find an optimum, it is good practice to check that its value, when the optimum is found, is acceptable. In choosing a material and shape to meet constraints on stiffness or on strength, the scale of the section has been treated as free, choosing a value that meets the constraint. One can imagine circumstances in which this might not be acceptable — when, for instance, the outer diameter d of a tube could be chosen freely provided it was less than a critical value d_c ; or when, to take another example, the width w of a beam was genuinely free but the height h free only so long as it was less than h^* . Dimensional constraints of this sort can change the index and the way it is used. The methods developed so far can be extended to include them.

For solid sections (cylinders, square sections) a dimensional constraint leads to a simple minimum limit for modulus or strength. Take bending stiffness as an example. The stiffness of a beam is:

$$S = \frac{C_1 EI}{\ell^3} = \frac{C_1 \pi r^4 E}{4\ell^3} \quad (\text{A7.1})$$

(using $I = \pi r^4/4$). If there is an upper limit on r then for the stiffness constraint to be met E must exceed the value

$$E = \frac{4S\ell^3}{C_1 \pi r^4} \quad (\text{A7.2})$$

Materials with lower moduli than this are excluded.

Limits for E for shaped sections are derived in a similar way. We take the tube as an example. Its bending stiffness is

$$S = \frac{C_1 EI}{\ell^3} = \frac{C_1 E}{\ell^3} \pi r^3 t = \frac{C_1 r^4 E}{\ell^3 \phi} \quad (\text{A7.3})$$

(using $\phi = r/t$). An upper limit on the radius leads to the limit

$$E = \frac{S\ell^3\phi}{C\pi r^4} \quad (\text{A7.4})$$

Only materials with moduli greater than this are candidates.

Constrained shapes

Constrained shapes appear when one dimension of the section is limited by the design. The idea is shown in Figure 7.14. When a 'free' shape changes scale, all the dimensions of its section scale by the same factor, as in Figure 7.1. When a constrained shape changes scale, all dimensions in one direction remain fixed, all those in the other scale by the same factor (Figure 7.14(a) and (b)). The constraint changes the material index.

When the width is constrained, we can no longer define ϕ by using a solid cylindrical section as the standard to which the other shapes are normalized. Instead — and in the same spirit as

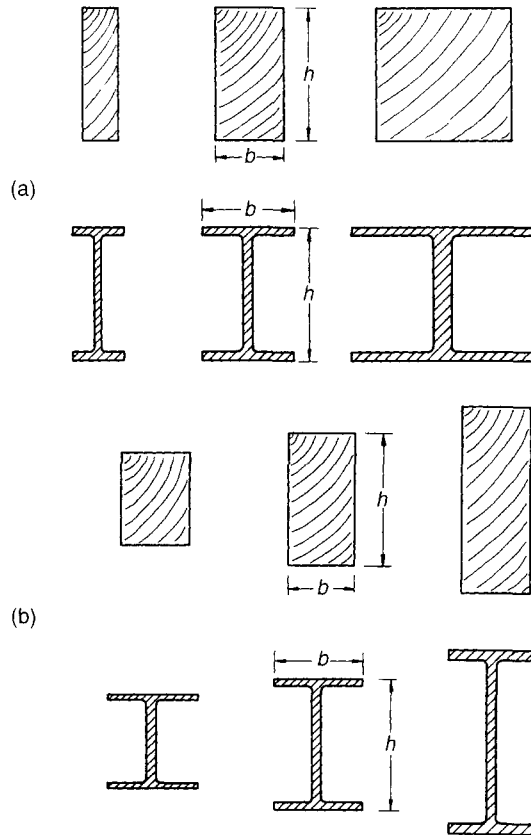


Fig. 7.14 A constrained section-shape is one in which the design fixes one dimension, but for which the other is free; all lengths in this direction change in proportion when the section changes size. It contrasts with a free shape (Figure 7.1) in which all dimensions change in proportion when the section changes in size. At (a) the height h is constrained; at (b) the width b is constrained.

before — we use the simplest solid shape that allows one dimension to be held fixed while leaving the other free: a flat plate of thickness t , width b and length ℓ . Its area A , its second moment I , and its section modulus Z are given in terms of its height t and its width b by (Table 7.1)

$$\begin{aligned} A^o &= tb \\ I^o &= \frac{bt^3}{12} \\ Z^o &= \frac{bt^2}{6} \end{aligned} \tag{A7.5}$$

Sections with constrained height, loaded in bending

The shape factor for elastic bending is defined, as before, as the ratio of the stiffness of the plate before (S_B^o) and after (S_B) ‘structuring’. ϕ_B^e now become

$$(\phi_B^e)_b = \frac{S_B}{S_B^o} = \frac{EI}{E^o I^o} \tag{A7.6}$$

(using $I = bt^3/12$). The stiffness of the plate is

$$S = \frac{C_1 EI}{\ell^3} = \frac{C_1 \phi_B^e E b t^3}{12 \ell^3} \tag{A7.7}$$

and its mass is $m = bt\ell\rho$. Eliminating t gives

$$m = \left(\frac{12b^2 S}{C_1 t^3} \right)^{1/3} \ell \left(\frac{\rho}{E^{1/3}} \right)$$

The lightest plate is that made from the material with the largest value of the index

$$M = \frac{(\phi_B^e E)^{1/3}}{\rho} \tag{A7.8}$$

An example will illustrate its use. Consider a plate, initially solid and of thickness t and width b which is foamed to a height h (width and length held constant). The density falls from ρ to

$$\rho^* = \rho \frac{t}{h}$$

and the modulus falls from E to

$$E^* = E \left(\frac{t}{h} \right)^2$$

(the scaling law for the modulus of foams). The stiffness falls from

$$S^o = \frac{C_1 E^o I^o}{\ell^3} = \frac{C_1 E^o b t^3}{12 \ell^3}$$

to

$$S = \frac{C_1 E^* I^*}{\ell^3} = \frac{C_1 E^* b h^3}{12 \ell^3} = \frac{C_1 E b t^3}{12 \ell^3} \left(\frac{h}{t} \right)$$

giving, for

$$(\phi_B^e)_b = \frac{S_B}{S_B^o} = \frac{h}{t} = \frac{1}{(\rho^*/\rho)}$$

As before, we find that foaming imparts a shape factor equal to the reciprocal of the relative density.

Following the same procedure for strength gives

$$(\phi_B^f)_b = \frac{M_f}{M_f^o} = \frac{Z\sigma_y}{Z^o\sigma_y^o}$$

with associated index (for minimum mass) of

$$M = \frac{(\phi_B^f\sigma_y)_b^{1/2}}{\rho}$$